Supporting Information

Interface-Oriented Bridges toward Efficient Carbon-Based Perovskite Solar Cells

Yan Chen[a], Zhensang Tong[a], Feifei Ding[a], Huanyi Zhou[a], Ye Yang[a], JinYan Huang[a], Jianwu Wei[a], Qionghua Su[a], Zhihui Liu[a], HanChi Cheng[b]; Peican Chen[a]*, and Liya Zhou[a]**

[a]School of Chemistry and Chemical Engineering, Guangxi Key Laboratory of Electrochemical Energy Materials, State Key Laboratory of Featured Metal Materials and Life-cycle Safety for Composite Structures, Guangxi Colleges and Universities Key Laboratory of Applied Chemistry Technology and Resource Development, Guangxi University, Nanning 530004, China.

[b]Department College of Chemistry and Resource Engineering, Wuzhou University, Wuzhou 543003, China.

*Corresponding author

E-mail: zhouliyatf@163.com; peicanchen@gxu.edu.cn; chcjmsu@163.com

Experimental

Materials: The FTO conductive glass was purchased from Advanced Election Technology Co., Ltd. Lead iodide (PbI_2, 99.99%) was purchased from TCI. Methylammonium iodide (MAI, 99.99%) was purchased from Greatcell Solar. N, N-dimethylformamide (DMF, anhydrous, 99.8%), dimethyl sulfoxide (DMSO, anhydrous, 99.9%), ethyl acetate (EA, anhydrous, 99.8%), thioglycolic acid (TGA, 98%), urea (>99.5%), Tin (II) chloride dihydrate ($SnCl_2$•$2H_2O$, >99.99%), was purchased from Sigma-Aldrich. Potassium bisaccharate (PH, 98%) was purchased from Aladdin. The commercial carbon paste (DD-10) was purchased from Guangzhou Saidi Technology Development Co, Ltd. All the materials and reagents were used as received without any further purification.

FTO substrates preparation: The FTO glass was cleaned through ultrasonic cleaning by detergent, deionized (DI) water, acetone, isopropyl alcohol, and ethanol for 20 min, respectively. After drying by dry-air blowing, it was treated by UVO for 15 min before use.

Electron transport layer (ETL) fabrication: SnO_2 ETL was fabricated by chemical bath deposition (CBD) method. 5 mL HCl (37 wt%) was added into 400 mL deionized water, followed by 5 g urea, and 1.096 g $SnCl_2$•$2H_2O$ was dissolved in the solution, finally 100μL of thioglycolic acid was added. Then the as-cleaned FTO glass was placed into the solution for 3 h at 90 °C. Then it is ultrasonic cleaned by deionized (DI) water, dried by gas gun blowing, and followed by the annealing at 170 °C for 1 h, followed by spin-coating10 mM KCl in DI water at 3000 rpm for 30 s and annealing at 100 °C for 10 min. For modified ETL, different concentrations of PH dissolved in water solution were spin-coated on SnO_2 for 30 s at 3000 rpm, and the modified SnO_2 films were subsequently annealed for 5 min at 100 °C.

C-PSCs fabrication: Before device fabrication, the FTO/SnO_2 substrates were treated by UV illuminated for 3 min. 2.2M $MAPbI_3$ perovskite precursor solution was prepared by dissolving MAI and PbI_2 in DMF/DMSO (v: v =9:1). The precursor solution was stirred at 60 °C for 3 h. After being filtered with a 0.22-μm polytetrafluoroethylene

(PTFE) the precursor solution was spin-coating onto FTO/SnO_2 substrates in an ambient environment (RH 40-50%) at 3000 rpm for 30 s, and 300 μL anti-solvent of ethyl acetate was dropped at the last 15s. The perovskite films were annealed at 130 °C for 15 min. Finally, the carbon electrode was deposited by screen-printing a mixed carbon paste on the top of the perovskite layer, followed by drying at 120 °C for 10 min.

Material characterization

A powder X-ray diffraction (XRD) system (Smartlab3 KW) equipped with Cu Kα radiation was used to measure the crystal structure. The GIXRD measurement was carried out by Micromax-007HF equipment. A field-emission scanning electron microscope (SEM, Hitachi SU8220) was used to examine the film's surface and cross-section morphologies. A Shimadzu UV2600 spectrophotometer was used to analyze the light absorption of the perovskite layer. The steady-state fluorescence spectra were acquired using an Edinburgh FLS1000 fluorescence spectrometer excited by a 465 nm xenon lamp flame. A nanosecond pulse semiconductor exciter with a wavelength of 405 nm was utilized as the excitation source for the time-resolved photoluminescence decay (TRPL) spectrum test, and the signal was received by a PMT900 detector. X-ray photoelectron spectrometer (XPS) measurements were conducted on an ESCALAB250XI+ system (Thermo Fisher Scientific). Ultraviolet photoemission spectroscopy (UPS) was performed by X-ray photoelectron spectrometer (Thermo Fisher Nexsa). Fourier transform infrared (FTIR) spectra were measured using an FTIR spectrometer with a NICOLET IS 50 FTIR (Thermo Fisher Scientific). Electrochemical impedance spectroscopy (EIS) measurements of the solar cell devices were obtained in the dark at 0.9V using a CHI660E electrochemical workstation (CHI Instruments Inc.)

within the frequency range of 10^{-1}-10^{6} Hz. The surface roughness of films was measured by atomic force microscope (AFM, ParkNX20). Green light pulse diodes (0.05 s square pulse width, 100 ns rise and fall time) controlled by a fast solidestate switch were used as the perturbation source. The voltage dynamics on the resistors were recorded on a digital oscilloscope (Tektronix MDO3032). The transient absorption (TAS) measurements were performed using a fiber laser (1030 nm, 100kHz repetition rate, 9.5 μJ/pulse, YF-FL-10-100-IR, Yacto-Technology, China) as the laser source and a femto-TA100 spectrometer (Time-Tech Spectra, China). Sum frequency generation (SFG) vibrational spectroscopy was performed using a custom-designed system (EKSPLA Co, Lithuania) to detect polymer chain structure information.

Device characterization:

J-V characteristics were measured using a Keithley 2400 digital sourcemeter and a solar simulator (Zolix SS150) under standard simulated AM 1.5 illumination (100 mW cm^{-2}). The *J–V* curves were measured with a scanning rate of voltage interval of 100 mV and delay time of 1000 ms from 1.5 to -0.1 V (reverse) or from -0.1 to 1.5 V (forward). Cells were covered by a black metal mask with an active area of 0.04 cm^2. The external quantum efficiency (EQE) of the device was obtained by the EQE measurement system (Enli Tech). Electrical impedance spectroscopy (EIS) measurements of the solar cell devices were obtained in the dark at 0.9 V bias using a CHI660E electrochemical workstation (CHI Instruments Inc.) within the frequency range of 10^{-1}–10^{6} Hz.

SFG sample preparation: CBD method (preparation details have been shown in the experimental part) was used for deposition at 90 °C for 8 hours, followed by annealing at 170 °C for 1h. Spin coating PH solution 1500rpm for 30 s, annealing at 100 °C for 5min.

***Computational details*:** The electrostatic surface potential was calculated by DMol3 code in Materials Studio. The projector-augmented wave method (PAW) was used to describe the interaction between electrons and ions, and the Perdew-Burke-Ernzerhof (PBE) functional of the generalized gradient approximation (GGA) method was used to describe the electron exchange correlation potential. The truncation energy of the plane wave function was set to E_{cut} = 571.4 eV. The convergence values of energy are set to 1E-6 eV.

***Time-resolved photoluminescence (TRPL) Measurement*:** Fitting parameters of the bi-exponential decay function in TRPL spectra of the corresponding perovskite films deposited on the glass substrate using a 405 nm excitation light source. The results are fitted with the bi-exponential decay Eq. (S1):

$$R(t) = A_1 \exp(-t / \tau_1) + A_2 \exp(-t / \tau_2) \quad \text{(S1)}$$

and the τ_{ave} is calculated by Eq. (S2):

$$\tau_{ave} = (A_1\tau_1^2 + A_2\tau_2^2)/A_1\tau_1 + A_2\tau_2 \quad \text{(S2)}$$

where A_1 and A_2 represent the corresponding decay amplitudes, while τ_1 and τ_2 represent the decay time constants.

***Trap Density Measurement*:** Calculated results of defect density (N_t) of the pristine and AS-modified devices from the *J-V* curves of SCLC measurements are shown in Figure 5a. The N_t is calculated by Eq. (S4):

$$N_{(t)} = \frac{2\varepsilon_r \varepsilon_0 V_{TFL}}{qL^2} \tag{S3}$$

where ε_r is the relative dielectric constant, ε_0 is the vacuum permittivity, V_{TFL} is the trap-filled limit voltage, q is the elementary charge, and L is the thickness of the perovskite layer.

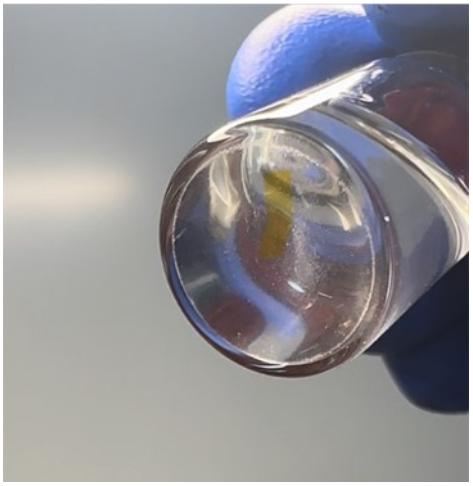

Figure S1. The suitability of PB in the DMF/DMSO solvent mixture.

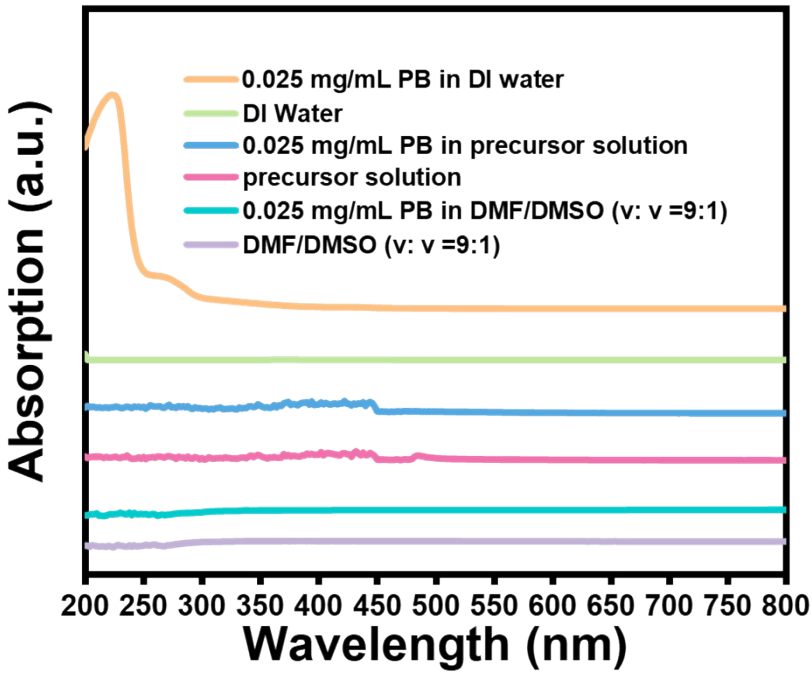

Figure S2. The UV absorption spectra of PB in DI water, the perovskite precursor solution, and the DMF/DMSO solvent mixture.

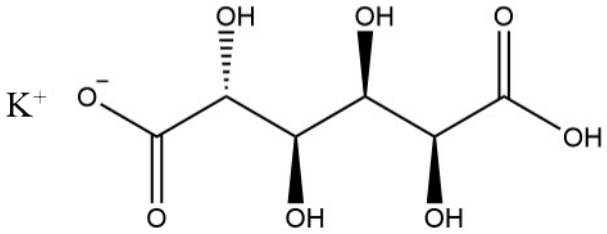

Figure S3. The molecular structure of Potassium bisaccharate

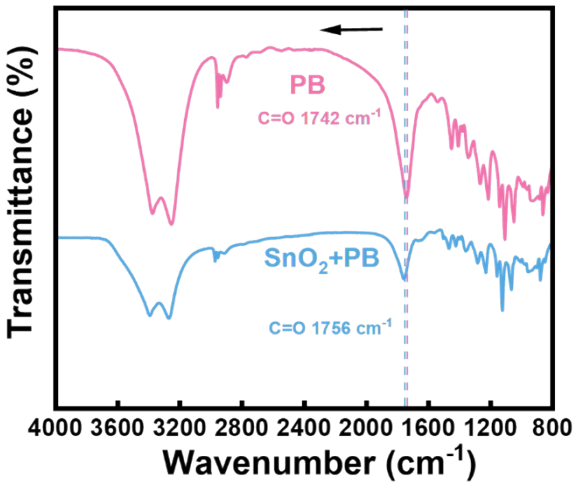

Figure S4. FTIR spectrum in the range of 800–4000 cm^{-1} of SnO_2+PB and PB.

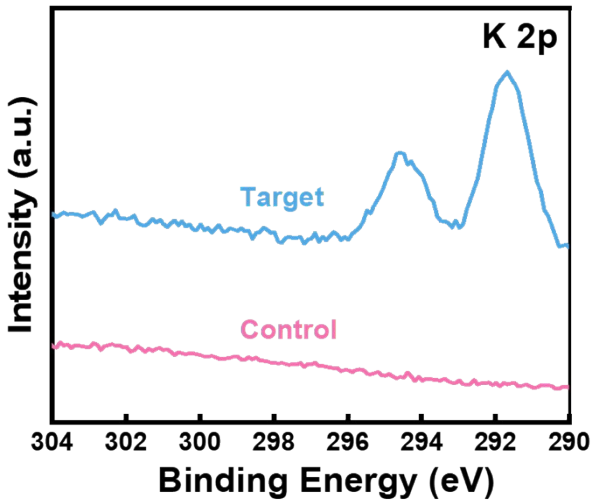

Figure S5. XPS spectrum of K 2p of. the pristine and PH-modified perovskite films.

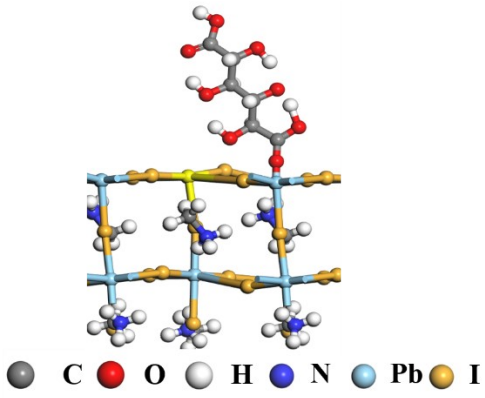

Figure S6. the adsorption energy of PB on $MAPbI_3$

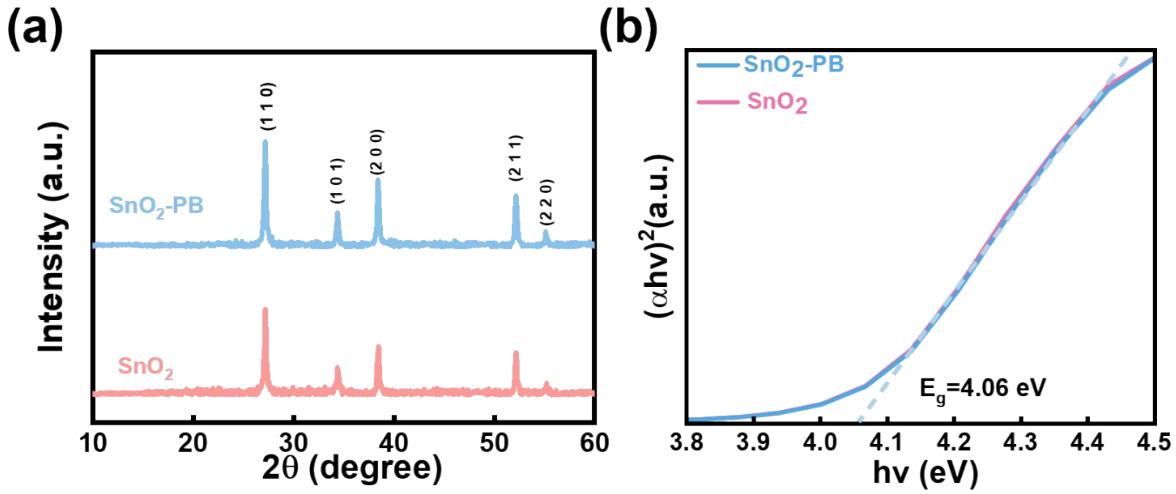

Figure S7. (a) XRD patterns for the pristine and PB-modified SnO_2 films, (b) Tauc plot of the pristine and PB-modified SnO_2 films.

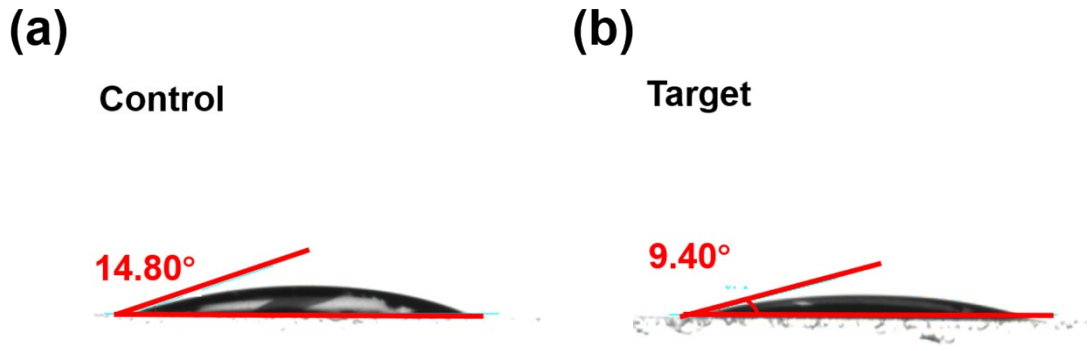

Figure S8. DMSO/DMF contact angles of (a) pristine and (b) modified SnO_2 films.

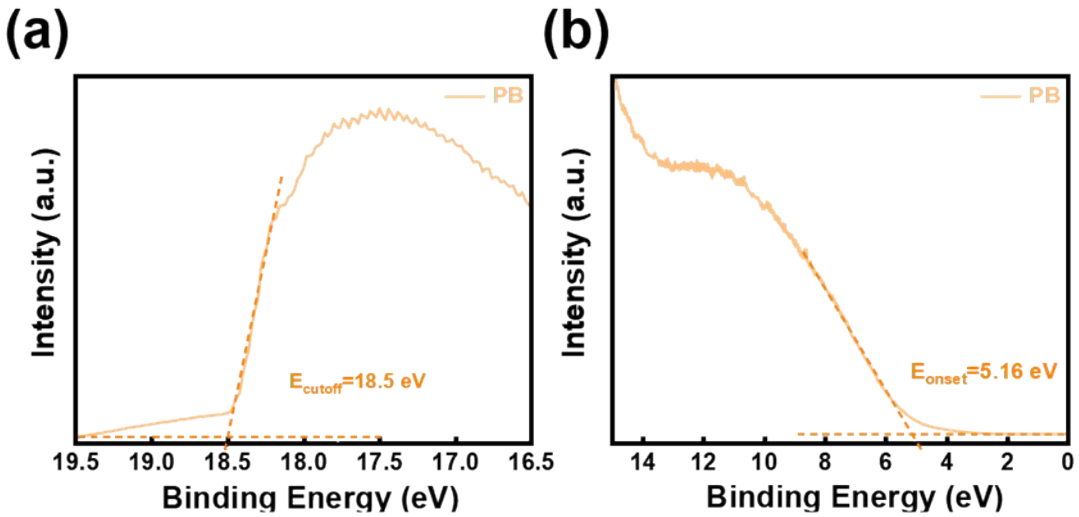

Figure S9. (a)and (b) The UPS spectra of PB.

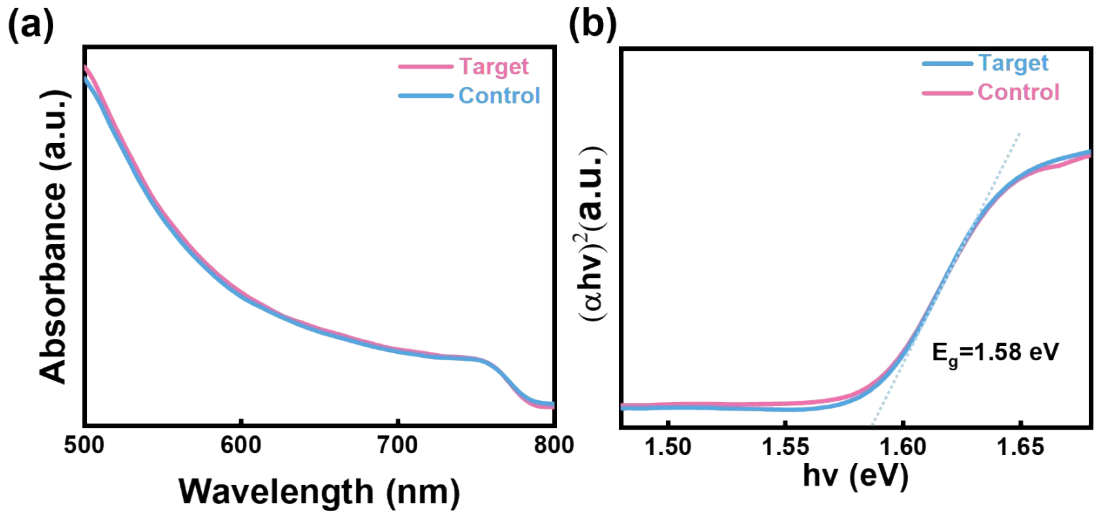

Figure S10. (a) UV-vis absorption spectra of the pristine and PB-modified perovskite films, (b) Tauc plot of the pristine and PB-modified perovskite films.

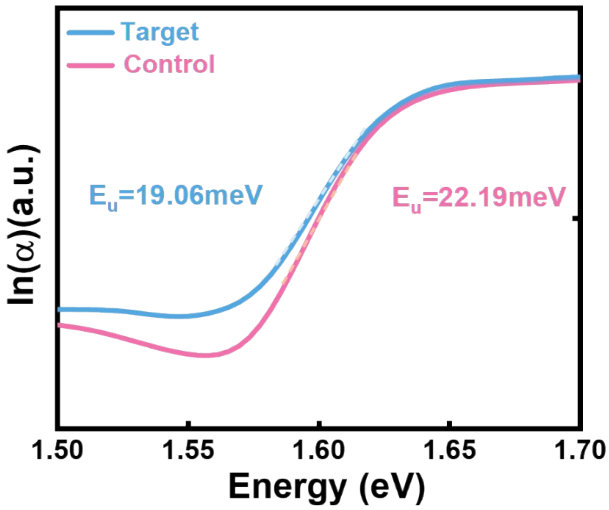

Figure S11. Logarithm of absorption coefficient α versus photon energy for perovskite films based on SnO_2 and SnO_2-PB.

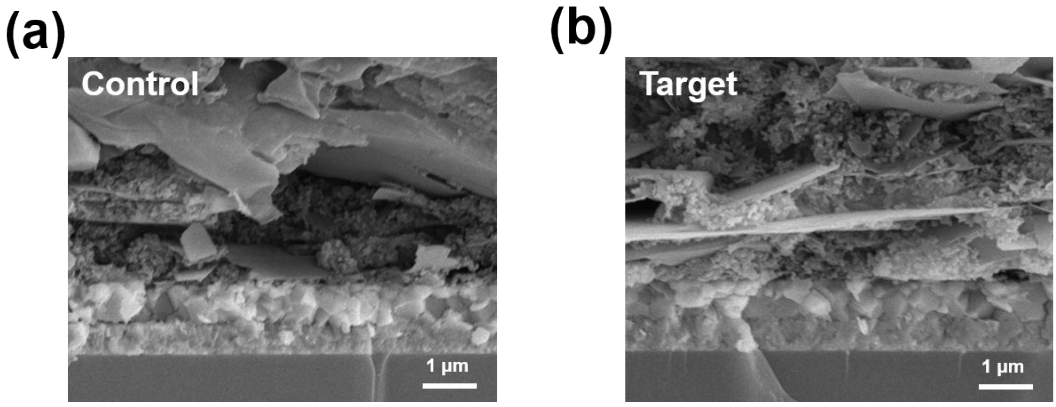

Figure S12. (a) Cross-sectional SEM images of FTO/SnO_2/perovskite and (b) FTO/SnO_2/PB/perovskite films.

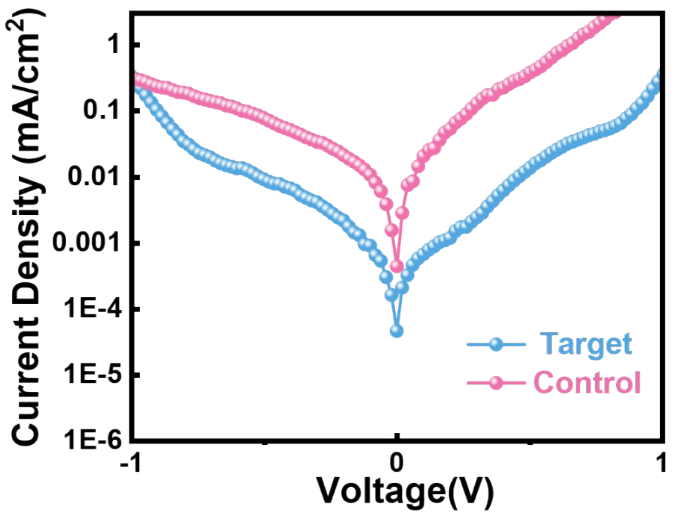

Figure S13. Curve of dark *J-V* for the pristine and PB-modified devices.

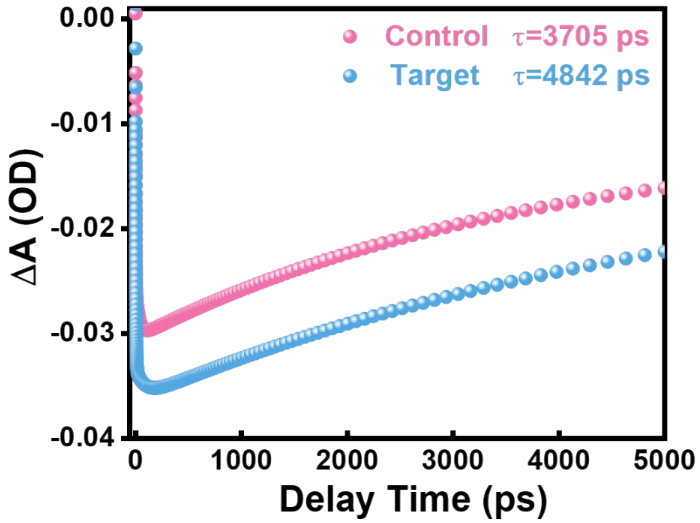

Figure S14. The bleach recovery kinetics for the pristine and PB-modified perovskite films following the excitation at probe wavelength.

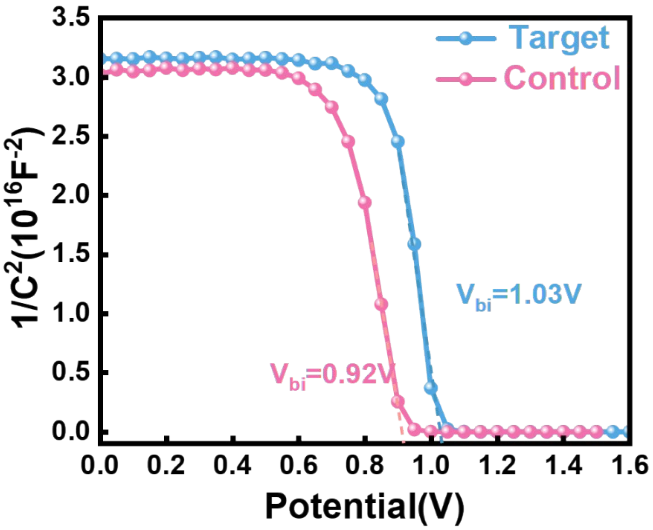

Figure S15. Mott-Schottky analysis at 1000 Hz of the devices based on pristine and PB-modified perovskite films.

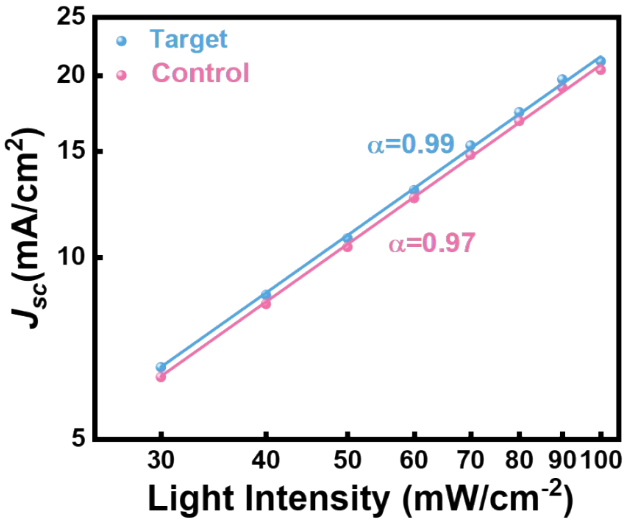

Figure S16. The relationship of *J*sc with respect to light intensity for the pristine and PB-modified perovskite films.

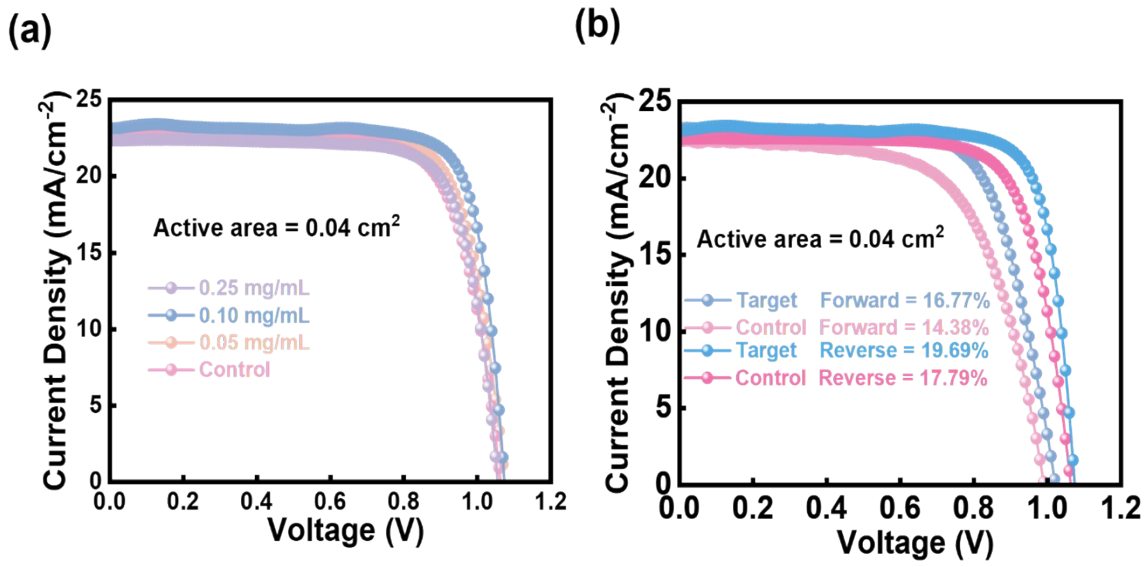

Figure S17. (a) *J-V* curves of C-PSCs using different concentrations of pristine and PB-modified device *J-V* curves, (b) The reverse and forward scans measure the best pristine and PH-modified device *J-V* curves.

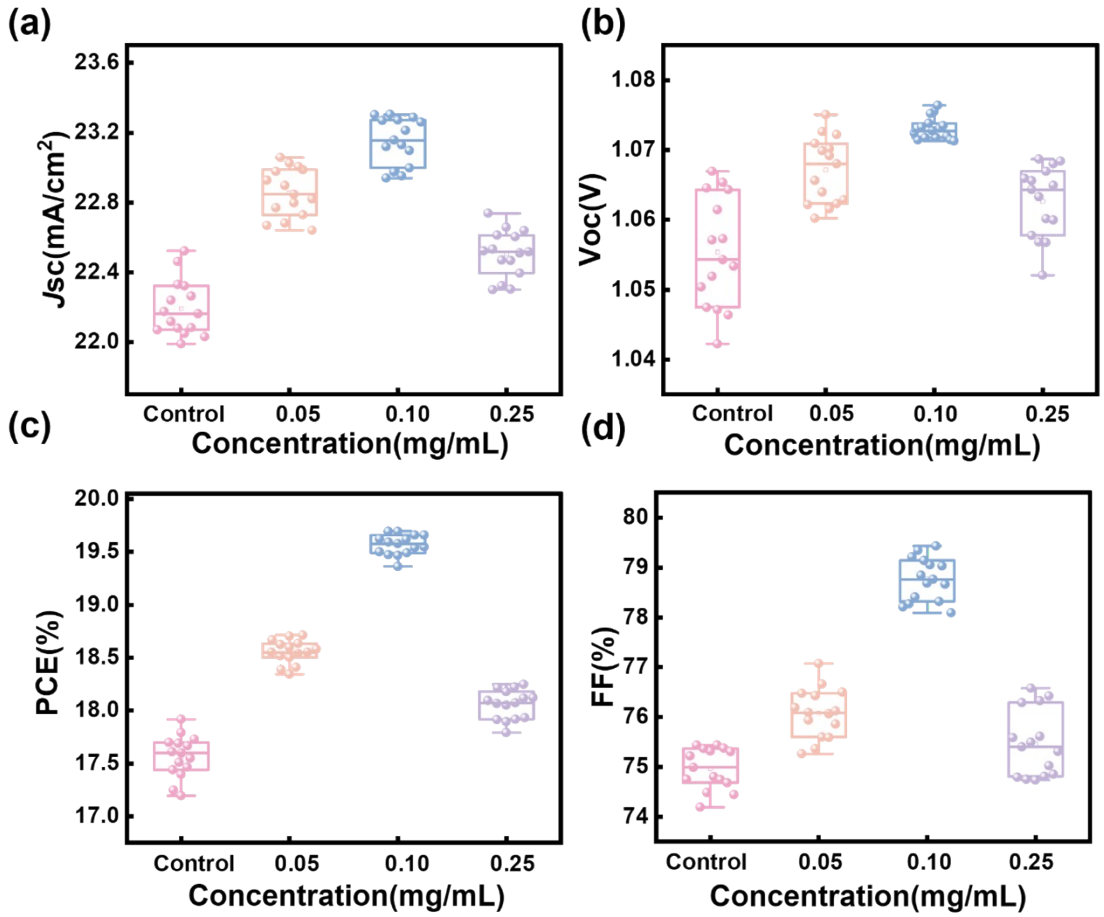

Figure S18. (a) *J*sc, (b) V_{oc}, (c) PCE, and (d) FF photovoltaic parameters for the PSCs modified by different PH concentrations ratios.

Table S1. Calculated relative amount of vacancy oxygen (O_v) and lattice oxygen (O_{lat}) for the SnO_2 and SnO_2/PB films by peak area in Figure 1c.

Devices	$O_{vacancy}$**(%)**	$O_{lattice}$**(%)**	O_v/O_L
SnO_2	37.20	62.79	0.59
SnO_2/PB	32.35	67.64	0.47

Table S2. The statistic parameters of perovskite films with or without AS modification time-resolved photoluminescence (TRPL) spectra fitted by bi-exponential function.

Devices	τ_1 **(ns)**	A_1	τ_2 **(ns)**	A_2	τ_{ave} **(ns)**
SnO_2/PVSK	9.23	0.48	508.98	0.47	499.89
SnO_2/PB/PVSK	5.34	0.64	385.57	0.29	374.30

Table S3. Calculated parameters and trap density (N_t) of perovskite films based on the pristine and PB-modified.

Devices	$\mathbf{V_{TFL}}$	***L* (nm)**	$\boldsymbol{\varepsilon_r}$	$\boldsymbol{\varepsilon_0}$**(F cm $^{-1}$)**	$\boldsymbol{N_t}$ **(cm $^{-3}$)**
SnO_2	0.40	880	28.8	8.85×10^{-14}	1.64×10^{15}
SnO_2/PB	0.32	880	28.8	8.85×10^{-14}	1.31×10^{15}

Table S4. Fitting results of the Nyquist plots of PSCs with and without PB modification.

Devices	R_s **(Ω)**	R_{rec} **(Ω)**
SnO_2	71.92	5032
SnO_2/PB	69.85	16703

Table S5. Fitting parameters of the decay lifetime by using a three-exponential equation obtained from the TAS measurements of the pristine and PB-modified perovskite films without an HTL layer based on FTO.

Device	t_1 (ps)	A_1	t_2 (ps)	A_2	t_3 (ps)	A_3	t_{avg} (ps)
Control	1.671	0.033	33.523	0.004	3694.550	-0.019	3705.523
Target	3.09	0.045	74.861	0.003	4842.250	-0.023	4857.742

Table S6. Photovoltaic parameters of the best performing control and target devices measured under both reverse and forward voltage scans.

Device	V_{OC} (V)	J_{SC} (mA cm^{-2})	FF	PCE (%)	HI
Control	1.054	22.32	0.753	17.79	0.189
	0.990	22.03	0.682	14.96	
Target	1.075	23.27	78.68	19.69	0.148
	1.023	23.23	70.61	16.77	

The hysteresis index (HI) index was calculated from forward and reverse scans by the following formula:[1]

$$HI = \frac{PCE_{reverse} - PCE_{forward}}{PCE_{reverse}} \#$$

Table S7. Summary of the champion and average photovoltaic parameters of the devices modified by different concentrations of PB.

Devices		J_{SC} (mA/cm^2)	V_{OC} (V)	FF（%）	PCE (%)
0 mg/mL	Average	22.19 ± 0.33	1.055 ± 0.013	74.97 ± 0.78	17.56 ± 0.35
	Champion	22.52	1.064	74.75	17.91
0.05 mg/mL	Average	22.85± 0.21	1.066 ± 0.008	76.08 ± 0.99	18.55 ± 0.21
	Champion	23.02	1.075	76.66	18.7
0.1 mg/mL	Average	23.15 ± 0.15	1.073 ± 0.003	78.76± 0.67	19.57 ± 0.20
	Champion	23.27	1.075	78.68	19.69
0.25 mg/mL	Average	22.50 ± 0.23	1.062 ± 0.01	75.46 ± 1.11	18.05±0.26
	Champion	22.46	1.06	76.32	18.24